

Contents lists available at ScienceDirect

Reactive and Functional Polymers

journal homepage: www.elsevier.com/locate/react





Fibril size control, tensile strength, and electrical properties of cyclic polyacetylene

Yu-Hsuan Shen ^a, Rinku Yadav ^a, Alexander J. Wong ^b, Alex H. Balzer ^{c,d}, Thomas H. Epps III ^{c,d}, Brent S. Sumerlin ^{b,*}, Adam S. Veige ^{a,b,*}

- ^a Center for Catalysis, Department of Chemistry, University of Florida, P.O. Box 117200, Gainesville, FL 32611, United States
- ^b George & Josephine Butler Polymer Research Laboratory, Center for Macromolecular Science & Engineering, Department of Chemistry, University of Florida, P.O. Box 117200, Gainesville, FL 32611, United States
- ^c Center for Plastics Innovation (CPI), University of Delaware, 221 Academy Street, Suite 250, Newark, DE 19716, United States
- ^d Department of Chemical and Biomolecular Engineering, University of Delaware, 150 Academy Street, Newark, DE 19716, United States

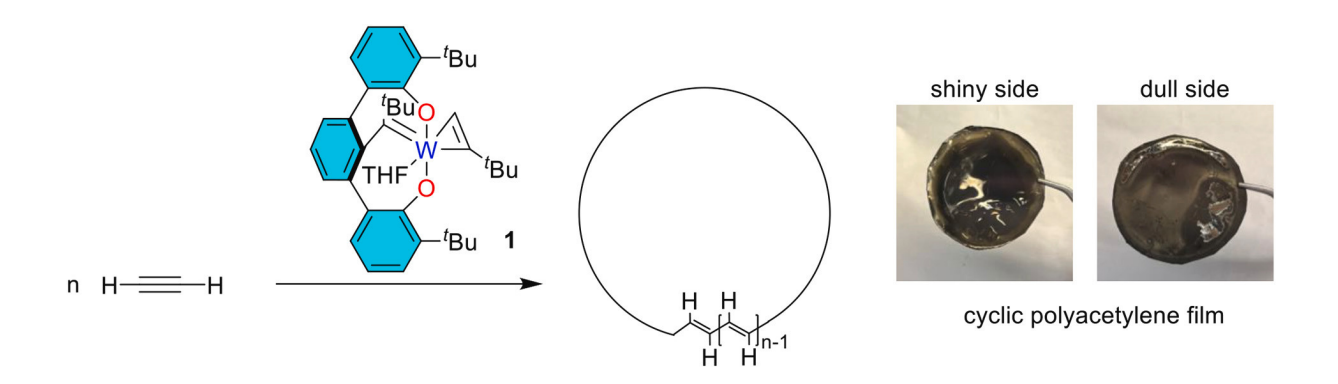
ARTICLE INFO

Keywords: Cyclic polymer Polyacetylene Conductive polymers Doping Increased conductivity Stretch polymer Morphology

Structure

ABSTRACT

We introduce a simplified synthesis of thick, flexible, cyclic polyacetylene films (c-PA) and study the relationship between stretchability and electrical conductivity of c-PA. Stretching the films 1.6 times their original length increases conductivity 5-fold.



^{*} Corresponding authors at: Department of Chemistry, University of Florida, P.O. Box 117200, Gainesville, FL 32611, United States. E-mail addresses: sumerlin@chem.ufl.edu (B.S. Sumerlin), veige@chem.ufl.edu (A.S. Veige).

1. Introduction

Linear polyacetylene (*l*-PA) is a quintessential flexible conducting organic polymer. Natta, in 1958, was the first to report the polymerization of acetylene to form black solids [1]. However, Shirakawa discovered the most widely employed method for synthesizing *l*-PA, involving the formation of a thin film [2,3]. By doping these *l*-PA films with halides or arsenic pentafluoride, conductivity reached levels comparable to metals [4–9]. This metallic behavior arises from the degenerate ground-state configurations of *trans-l*-PA [10–15], and the doping of films serves to mitigate the energy gap arising from bond alternation [16,17]. Although various indirect methods for *l*-PA synthesis yield materials that offer improved processability, *l*-PAs resulting from these methods tend to exhibit diminished conductivity compared to polyacetylene directly synthesized from acetylene [18–25].

l-PA is arguably the most well-studied conducting polymer, with thousands of articles reporting its spectroscopic characteristics, derivatives, applications, solid-state physics, alternative syntheses, mechanical properties, and doping. In contrast, the cyclic version of polyacetylene, c-PA, recently reported by our group [26], has yet to be interrogated extensively. Catalyst 1 polymerizes acetylene in a ring-expansion polymerization (REP) [27] to produce pure trans-c-PA with minimal defect concentrations. Evidence for a cyclic architecture comes from atomic force microscopy (AFM) of bottlebrush derivatives. Furthermore, computational findings strongly indicate that c-PA adopts an all-trans conformation. When subjected to iodine (I2) doping, c-PA films demonstrate noteworthy electrical conductivity at 398 (\pm 76) $\Omega^{-1}\text{cm}^{-1}$, in contrast to the conductivity of 179 (\pm 21) $\Omega^{-1}\text{cm}^{-1}$ exhibited by trans-l-PA synthesized in the same manner. This distinct difference highlights the considerable potential of c-PA in electronic applications.

It is challenging to ascertain the impact of a cyclic topology on the properties of c-PA relative to l-PA, because defects play an essential role in the expression of physical properties [28–35]. For example, enhanced stretching ratios in l-PA films also contribute to their amplified conductivities. Stretching l-PA orients the PA fibrils uniformly along the axis of the applied force, resulting in remarkable conductivities as high as $10^5~\Omega^{-1}\,\mathrm{cm}^{-1}$ [29,33,36]. Improving conductivity in polymers through the stretching of l-PA is a developing method in the field. The impact of orientation on conductivity in stretch-aligned cyclic polymers is unknown.

In this study, we present a simplified method for synthesizing thick and flexible films of c-PA and examine how stretching affects their electrical conductivity. Extending the films to $1.6\times$ their original length resulted in a fivefold increase in conductivity. Additionally, we address the issue of inconsistent material synthesis across different labs in the field of conducting polymers. Our straightforward synthesis and purification process aims to establish a reliable and reproducible method, facilitating future research and applications of c-PA.

2. Experimental

2.1. General considerations

All manipulations were conducted under an inert atmosphere using standard Schlenk or glovebox techniques. Toluene and tetrahydrofuran (THF) were degassed by sparging with high-purity argon and were dried using a GlassContour drying column. Acetylene was purchased from Airgas and passed through a column of activated carbon and 3 Å sieves placed in a cold trap (–78 °C, dry ice and acetone) prior to introducing into the reaction vessel. Complex 1 was prepared according to literature procedures [27]. A 150 mL sublimator was purchased from Chemglass Life Sciences, item number CG-3038-01. Titanium(IV) butoxide and triethylaluminium solution (25 wt% in toluene) were purchased from Millipore Sigma and used as purchased. Infrared spectra were collected on a Thermo Nicolet 5700 Fourier-transform infrared (FTIR)

spectrometer equipped with a single bounce, diamond-stage attenuated total reflectance (ATR) accessory.

2.2. Synthesis of c-PA fibrils

In a nitrogen-filled glovebox, a vial containing 4 mL of toluene was prepared, sealed with a septum, and secured with electrical tape. The vial was taken out of the glovebox, and the solution was sparged with acetylene for 5 min through a needle inserted into the septum. After sparging, the needle was removed, and the septum was securely covered with tape to prevent air entry. Finally, the vial was returned to the glovebox.

For dynamic light scattering (DLS) analysis, a 4 mL sample of the acetylene-saturated toluene solution was passed through a syringe filter and transferred into a cuvette. The cuvette was then sealed with a septum screw cap. A toluene stock solution of catalyst 1 (1 mg/mL) was prepared in the glovebox. Depending on the specific experiment, different volumes of the catalyst solution were taken into a syringe and then added to the cuvette just before conducting the DLS analysis.

For transmission electron microscopy (TEM), a 4 mL sample of the acetylene-saturated toluene solution was passed through a syringe filter into a vial. Different amounts of catalyst 1 stock solution in toluene (1 mg/mL) were added to the reaction according to the experimental requirements. The reaction was allowed to proceed for various time intervals, and then five drops of a 5 μL solution each were cast onto a TEM grid for imaging and analysis.

2.3. Synthesis of c-PA films

In a nitrogen-filled glovebox, 4.00 mL of catalyst 1 in toluene (5.00 mg/mL) was added to a flatbed 150 mL sublimator, and the solution was evenly coated at the bottom to form a layer of light-yellow catalyst solution. The sublimator was assembled, removed from the glovebox, and attached to a Schlenk line connected to the acetylene purification system. The tube connecting the sublimator to the Schlenk line was degassed three times to remove residual oxygen. A slight vacuum was applied to the sublimator, and acetylene gas was introduced. Slightly swirling the sublimator for the initial polymerization produced a black gel, and heat was generated. After 15 min of exposure to acetylene, the sublimator was evacuated and taken back into the glovebox. The resulting polyacetylene film was wetted with THF and peeled off from the bottom of the sublimator. The film was washed with THF and pentane several times until the resulting solutions turned colorless and dried under a dynamic vacuum. This washing and drying cycle was repeated three times to yield c-PA as a thick black film. (646 mg) FTIR (Fig. 2): 3010 cm^{-1} , =C-H stretch; 1010 cm^{-1} , trans = C-H out of plane bending.

2.4. Synthesis of l-PA films

The synthesis of l-PA films was carried out using a slightly modified version of Shirakawa's method, resulting in cis/trans mixtures [3]. In a 150-mL flatbed sublimator, 1.50 mmol of titanium(IV) butoxide (0.500 mL), 4.50 mmol of triethylaluminum (2.30 mL of 25% wt solution in toluene), and 4.00 mL of toluene were mixed at room temperature for 20 min. The sublimator was removed from the glovebox, connected to a Schlenk line, and cooled using a dry-ice/methanol mixture before evacuation. After reaching a constant temperature, acetylene was introduced into the sublimator, and the formation of a polyacetylene film was observed immediately. The sublimator was left under acetylene for 1 h. After this time, the sublimator was evacuated and returned to the glovebox at room temperature. The resulting polyacetylene film was washed with THF and toluene multiple times until the solutions turned colorless. The film was then dried under a dynamic vacuum for approximately 15 min to yield cis/trans-l-PA as a lustrous film (150 mg). The film was heated at 180 °C for 30 min to isomerize the cis/trans-l-PA film from *cis:trans* = 55:45 to \geq 99% *trans-l*-PA [26]. FTIR (Fig. 2): 3010 cm⁻¹, =C-H stretch; 1010 cm⁻¹, *trans* = C-H out of plane bending. The transmittance for *trans* = C-H and cis = C-H out of plane bending (740 cm⁻¹) is 40.1% and 43.2%, respectively. The *cis/trans* ratio was calculated to be 55:45, as *cis*% = 100[1.30A_{cis}/(1.30A_{cis} + A_{trans})] [3].

2.5. Doping of c-PA and l-PA films

The PA films were introduced to I_2 in an evacuated iodine chamber for 3 h. After the doping process, excess I_2 was removed by subjecting the films to a dynamic vacuum overnight. The iodine doping weight percentages were calculated based on the weights before and after doping.

2.6. DLS measurements

Dynamic light scattering (DLS) was performed with a non-invasive backscatter system (Malvern Zetasizer Nano ZS) with a measuring angle at 173° and adjustable focus. The samples were analyzed in a quartz fluorometer cuvette with a septum screw top purchased from Starna Cells, Inc. DLS was performed at 25 $^\circ$ C every 3.5 min, and the size distributions reported were averaged over five experiments.

2.7. TEM imaging

Transmission electron microscopy (TEM) images were obtained on a FEI TALOS F200I S/TEM. The operating voltage was 80 kV with an S-FEG Schottky field emission gun.

2.8. DMA measurements

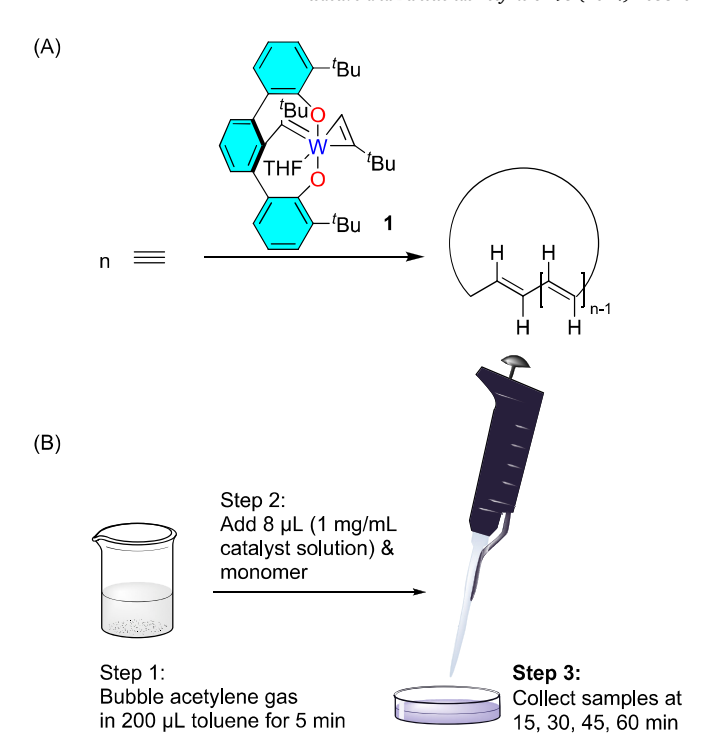
Dynamic mechanical analysis (DMA) was measured with a TA Instruments Dynamic Mechanical Analyzer (DMA Q800). The samples were clamped in a film tension clamp, and force was ramped at $0.05~\rm N/min$ while the stress and strain were monitored. A steady argon flow was plumbed into the top of the DMA Q800's furnace lid to keep the samples from oxidizing. Samples were removed and stored under argon once a force of 18 N was applied or the sample yielded, whichever condition was reached first.

2.9. SEM imaging and EDS analysis

Scanning electron microscopy (SEM) images were obtained on a Tescan MIRA3 scanning electron microscope. The operating voltage ranged from 5 to 15 keV with a Schottky field emission gun ZrO/W source. Energy-dispersive X-ray spectroscopy (EDS) images were collected using EDAX Octane Pro energy-dispersive spectroscopy system.

2.10. SAXS and WAXS analysis

Small-angle x-ray scattering (SAXS) and wide-angle x-ray scattering (WAXS) were conducted on a Xenocs instrument with a sealed-tube X-ray source (Cu K α , $\lambda=1.54$ Å) operating at 2.0 kW with a Dectris Pilatus 300 k 2-D detector (3 panels, 48-chip array with 1 dead chip, 1 pixel = $172\times172~\mu\text{m}^2$). The path tubes were held under dynamic vacuum to reduce scattering from air, and sample strain was controlled using a Linkam TST350 stage operated inside the SAXS/WAXS sample chamber under dynamic vacuum. Sample-to-detector distance was 72 mm for WAXS, 1200 mm for small-angle distance (SAXS2), and 2300 mm for smaller-angle distance (SAXS3). All experiments were conducted at room temperature (20-22_°C). All samples were measured with two exposures of 5 min (WAXS) and 1 min (SAXS2, SAXS3), each at different detector positions, and stitched together using the instrument's lineeraser function to remove blind spots in the 2-D spectrum. All 2-D



Scheme 1. (A) c-PA synthesis via ring-expansion polymerization with catalyst 1; (B) Synthetic scheme for the preparation of c-PA fibrils.

scattering data were azimuthally integrated, resulting in plots of scattered intensity vs. angle (2Θ) or scattering vector (q).

2.11. Conductivity and thickness measurements

The resistivity of the polyacetylene films was measured on a Signatone Pro4–4400 4-point probe station equipped with a Keithley 2400 source meter. The thickness of the films was measured using a Tencor Alpha-Step AS500 profilometer. The resistivity of the polyacetylene films was obtained by measuring the sheet resistivity with the 4-point probe station and determining the thickness with the profilometer. The conductivity of the films was calculated as the reciprocal of the resistivity.

3. Results and discussion

3.1. Synthesis of c-PA fibrils

Scheme 1 A depicts the Ring Expansion Polymerization (REP) [37–44] of acetylene to produce cyclic polyacetylene (c-PA) with catalyst 1 [27]. Sparging 5 mL of toluene with acetylene gas for 5 min produces an acetylene-saturated solution. Combining 200 μ L of the acetylene solution with varying volumes of catalyst solution (4, 8, 16, and 24 μ L) generates cyclic polyacetylene with variable fibril sizes. Investigation of the fibril dimensions by DLS reveals a distinct growth pattern, escalating with both prolonged reaction time and higher catalyst concentration (Fig. 1). At 40 min, a significant increase in particle size was observed when utilizing both 4 and 24 μ L of catalyst 1 solution. The particle size expanded from ~870 to ~1900 nm, clearly indicating catalyst concentration directly impacts the growth of particles.

Fig. 2 shows a series of TEM images depicting the fibrils generated by mixing 200 μ L of acetylene-saturated toluene solution with 8 μ L of catalyst 1 solution at different reaction times. In these images, it is evident that a thin layer of fibrils appears on the surface at 15 min. As the reaction time increases, the fibrils gradually thicken, eventually forming a film-like structure on the surface with only a few protruding fibrils [45,46].

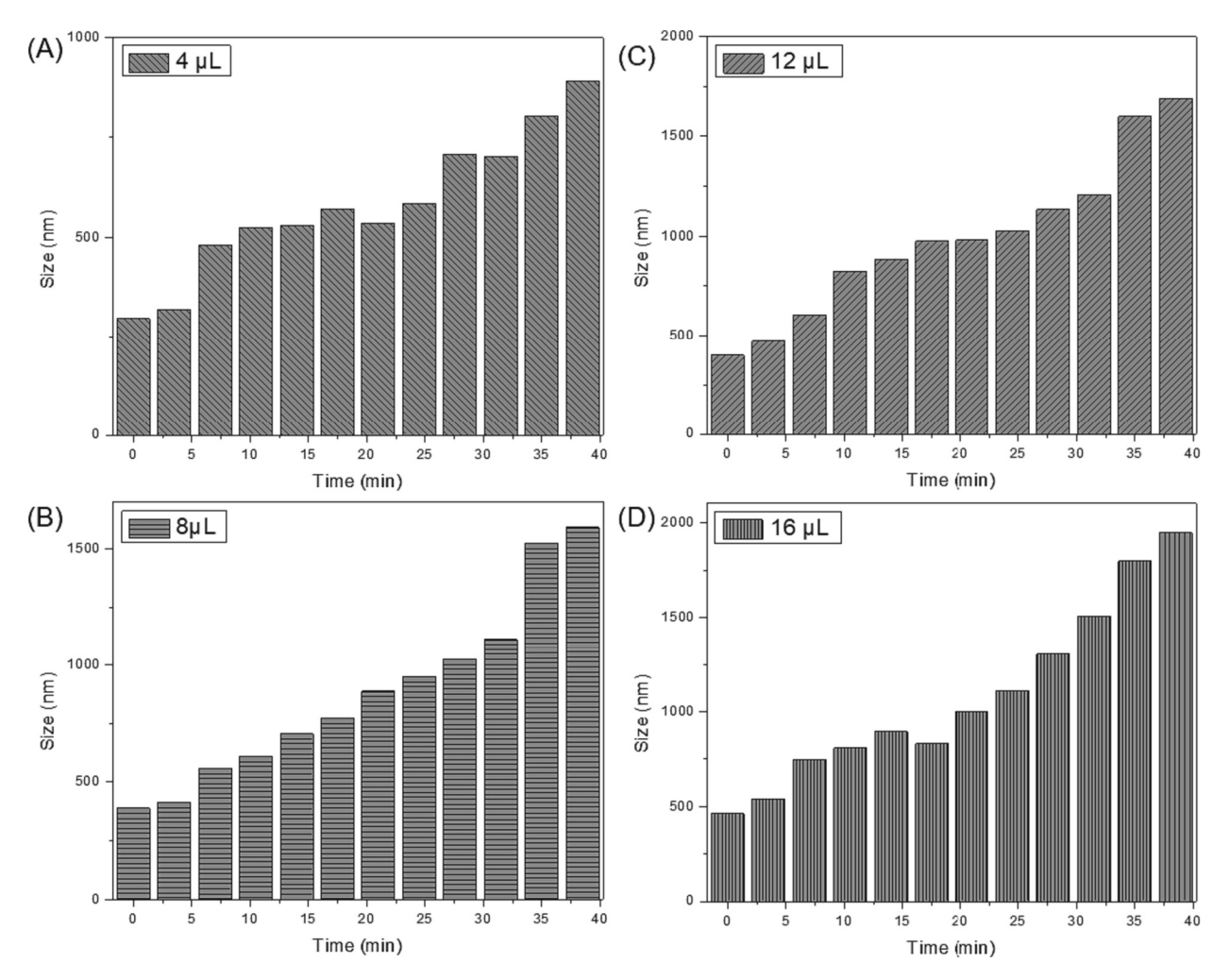


Fig. 1. Hydrodynamic diameters from dynamic light scattering showing particle size growth with (A) 4 μ L, (B) 8 μ L, (C) 12 μ L, (D) 16 μ L of catalyst 1 solution.

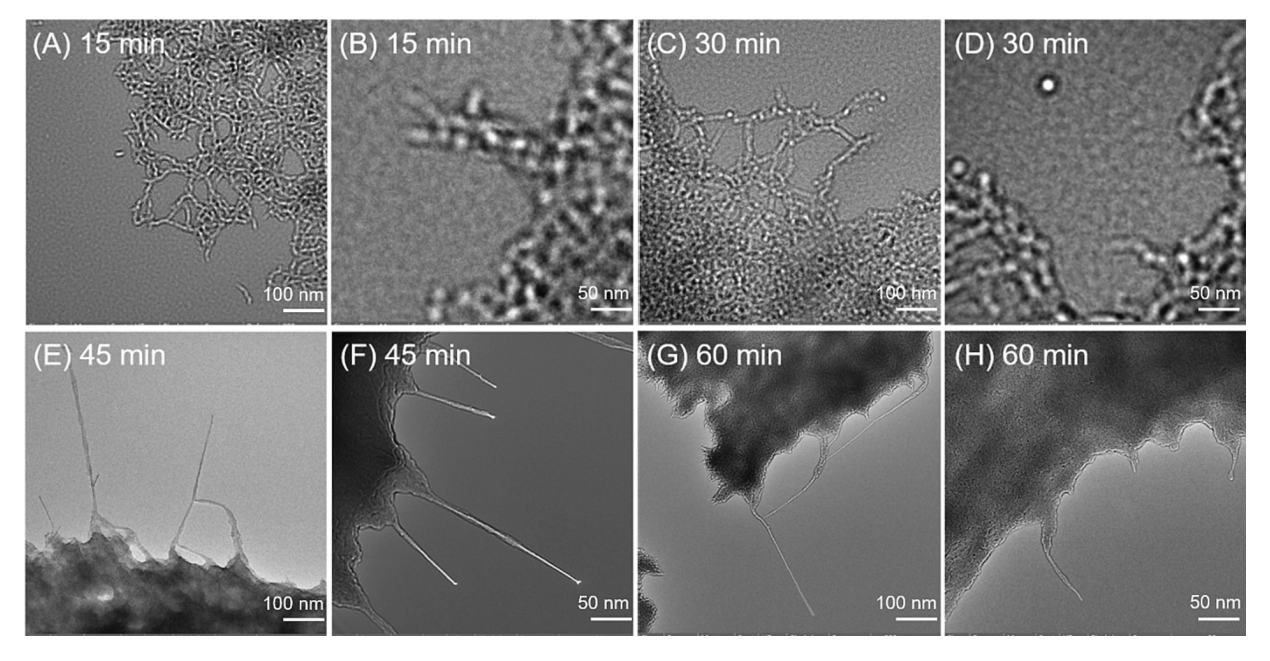
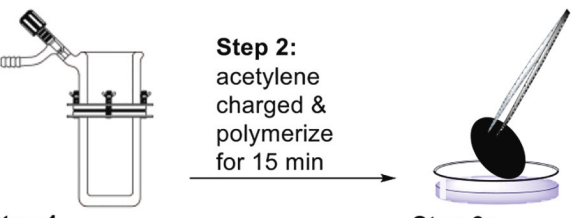


Fig. 2. TEM images of the c-PA growth using 8 μ L of catalyst 1 solution at (A)(B) 15 min, (C)(D) 30 min, (E)(F) 45 min, and (G)(H) 60 min.



Step 1: 4 mL (5 mg/mL catalyst solution) in toluene

Step 3: peel off the *c*-PA film and wash it with THF

Scheme 2. Synthetic scheme of *c*-PA films.

3.2. Synthesis of c-PA films

Treating 4.00 mL of light-yellow catalyst 1 solution (5 mg/mL in toluene) in a sublimator with acetylene at room temperature initiates REP of acetylene (Scheme 2). Carefully swirling the sublimator during the first minute of polymerization is crucial for the formation of the thick c-PA film. Upon initiation, small blue particles form immediately, followed by the development of a black lustrous gel-like film once the acetylene meets the catalyst solution. Introducing acetylene for an additional 15 min results in a significant increase in film thickness and generates heat. Washing the c-PA film with THF repeatedly until the solution turns colorless, and drying the film under a dynamic vacuum removes residual catalyst and affords a gelatinous black stretchy film. The films become solid and flexible after being dried for 1 h. Similar results were demonstrated in previous cases involving l-PA films

[47,48]. Film thickness is directly proportional to the volume of catalyst solution used. Fig. 3 displays a black flexible film made using this method. These films are notably thicker than the c-PA films reported previously [26]. Fig. 4 depicts the IR spectrum of the c-PA films. The spectrum reveals a strong trans = C-H out-of-plane bending at $1010\,\mathrm{cm}^{-1}$ and a weak = C-H stretching vibration at $3010\,\mathrm{cm}^{-1}$.

A $Ti(O^nBu)_4/AlEt_3$ solution exposed to acetylene produces linear polyacetylene (l-PA) films with varying degrees of cis:trans content at different temperatures. At room temperature, the cis:trans content is 58:42, respectively; upon heating the films at 180 °C, the films isomerize to >99% trans [49]. Previous studies suggest that trans-l-PA films are rigid and challenging to stretch, whereas increasing the cis content results in more elastic and stretchable polyacetylene films [50]. Following a similar approach by Ito and Shirakawa [3], exposing the $Ti(O^nBu)_4/AlEt_3$ solution to acetylene in a sublimator for 1 h generates a cis/trans-l-PA film. Heating the l-PA film at 180 °C for 30 min isomerizes the film from 45% to $\geq 99\%$ trans-l-PA (ratio determined according to literature [3]). Fig. 4 displays FTIR spectra of c-PA and l-PA.

Previous studies on film stretching demonstrate that stretching l-PA films orients the fibrilchain axis [51,52]. Denko stretched l-PA films using clamps and a 660 g load at 130–160 °C in vacuo to $l/l_0 = 2.5$ (l_0 : initial length of the film; l: length after elongation) [53]. Shirakawa increased the ratio of l/l_0 to 4 during isomerization under stress with a tensile strength of 2.4 kg/mm² for a 96% trans-l-PA film [51]. Due to its cyclic topology, unique synthesis, and the fact it does not need to be heated to isomerize, c-PA exhibits lower levels of entanglement and crosslinking within its structure. Therefore, the polymer is more compliant, and stretching occurs at ambient temperature.

By carefully and slowly elongating the c-PA films by hand (avoiding

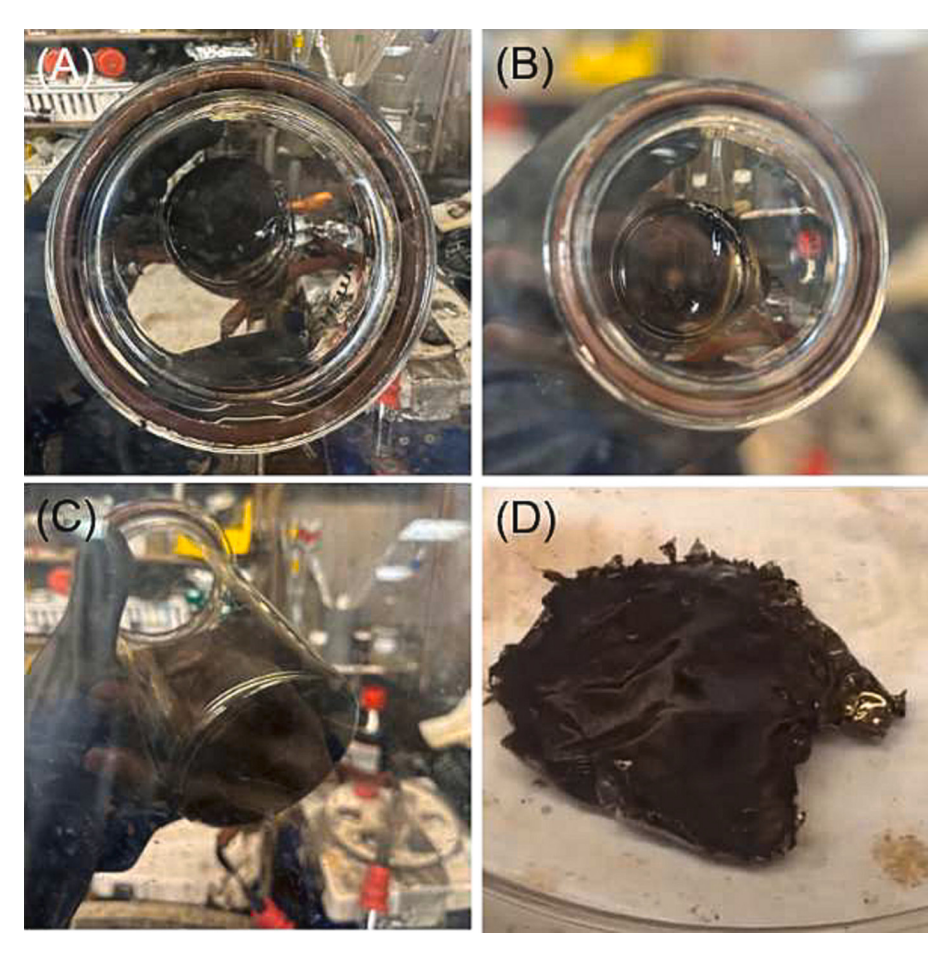


Fig. 3. Photographs of *c*-PA films. In (A) and (B), the film is observed from a top-down perspective in the reaction vessel; (C), the reaction vessel is presented in a side view, and (D), the film is depicted after being removed from reaction vessel.

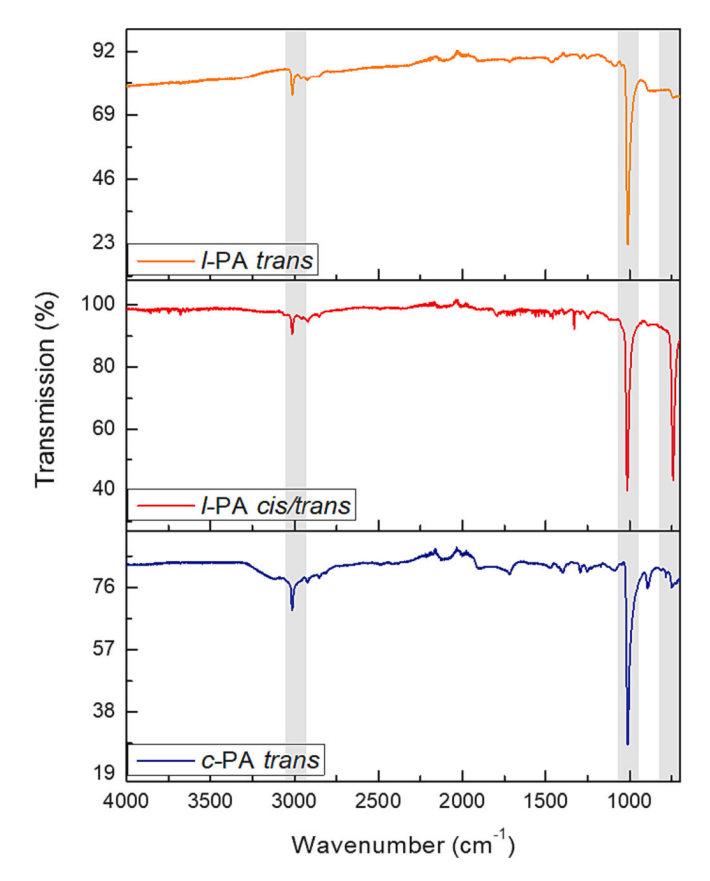


Fig. 4. FTIR spectra of the *c*-PA, *cis/trans-l*-PA, and *trans-l*-PA films. The important features are the strong = C–H out-of-plane bending at $1010\,\mathrm{cm}^{-1}(trans)$, and 740 $\mathrm{cm}^{-1}(cis)$ and the weak = C–H stretching vibration at $3010\,\mathrm{cm}^{-1}$.

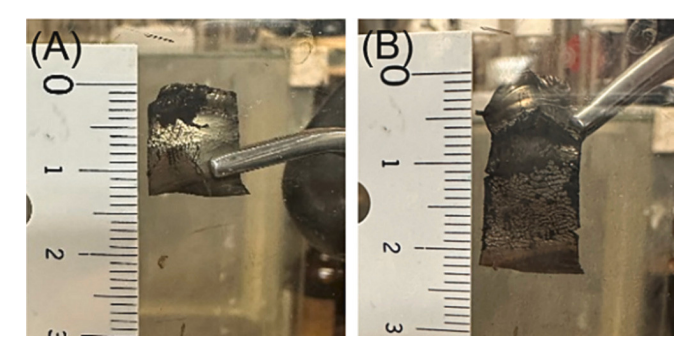


Fig. 5. Photographs of c-PA films (A) before and (B) after manual stretching.

Table 1Length of the *c*-PA films before and after manual stretching.

l _o (cm) ^a	1 (cm) ^b	l/l _o
2.4	3.1	1.3
1.7	2.5	1.5
1.2	2.2	1.8
1.5	2.5	1.7
1.4	2.1	1.5
1.7	2.7	1.6
1.8	2.7	1.5

^a Initial length of the film.

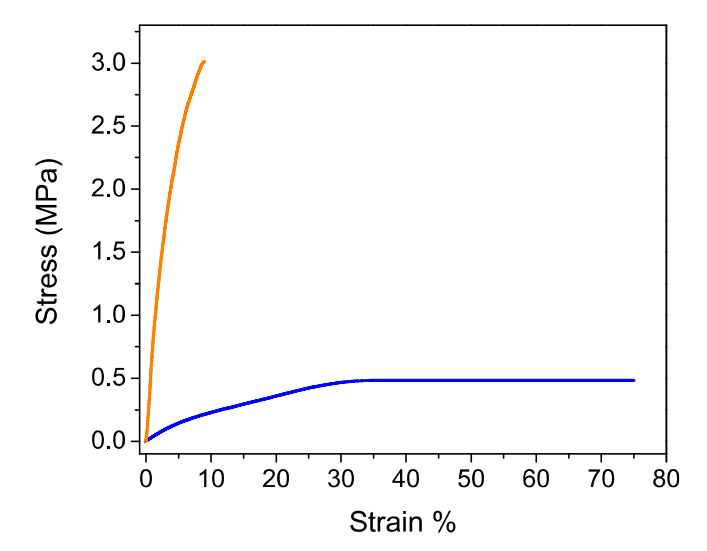


Fig. 6. The stress-strain curve of a thick (0.37 mm) c-PA film (blue) and a thin (3.0 \times 10⁻² mm) c-PA film (orange). (For interpretation of the references to colour in this figure legend, the reader is referred to the web version of this article.)

any tearing), the films stretch an average of 60%. Fig. 5A and B depict one of the c-PA films before and after stretching. The film elongates from 1.2 to 2.2 cm, giving an $1/l_0$ of 1.8. Consequently, the film thickness decreases from 42×10^{-2} mm to 5.4×10^{-2} mm after stretching. Table 1 demonstrates seven trials of manual stretching the c-PA films. Although stretching the gelatinous c-PA films by hand increases the length, this method is not uniform or quantifiable. Employing dynamic mechanical analysis (DMA) for more precise measurements addresses this issue.

Subjecting the *c*-PA films to increasing stress, measured as force per cross-sectional area [54], results in elongation in response to the applied force. Setting the force ramp to 0.05 N/min and applying constant argon flow during the DMA analysis, the *c*-PA films take up to 2 h to elongate and break. Fig. 6 depicts the stress-strain curve, indicating the *c*-PA films, on average, stretch by 75%, resulting in a l/l₀ of 1.75. Notably, the film thickness decreases from 0.37 to 0.038 mm at the fracture point. Despite elongation, the film retains its flexibility. In comparison, thinner *c*-PA films about 3.0×10^{-2} mm thick prepared according to previous literature exhibit a mere 8.9% stretch under a maximum force of 18 N, resulting in an elongation ratio (l/l₀) of 1.1 [26]. It is not possible to manually stretch the *l*-PA films by hand, with both the *cis/trans-l*-PA and *trans-l*-PA films retaining the same length before and after manually applying tensile force when no heat is applied.

Fig. 7 (A) and (B) illustrate the morphology of the film before the hand stretching process, showing the shiny side of the film, which is the side in contact with the acetylene atmosphere. Under magnification, the *c*-PA appears to have a distinctive popcorn-like structure, deviating from the spiderweb-like configuration of fibrils observed in the reported *l*-PA case [51] and the thin *c*-PA case [27]. Upon manual stretching, the *c*-PAs is stretched apart, and some wispy stripes were formed on the surface due to the stretchy and elastic texture of the film.

Fig. 8 presents the EDS results for the c-PA films. The analysis reveals the presence of only carbon and a minimal amount of oxygen atoms. This outcome indicates the successful removal of all catalyst ${\bf 1}$ employed in the polymerization process, and notably, no tungsten signals were detected in the analysis. Consequently, the c-PA film is confirmed to be composed solely of carbon and hydrogen atoms.

The WAXS traces of l-PA and c-PA both show a primary diffraction peak of $\sim 30^\circ$ and a secondary diffraction peak of $\sim 38^\circ$ (Fig. 9). For l-PA, the diffraction peaks at 29.4°, 35.8°, and 38.3° correspond to d-spacings of 3.0 Å, 2.5 Å, and 2.4 Å, respectively. The c-PA sample has a very similar trace with diffractions peaks at 31.2° and 40.1° corresponding to

^b Length after elongation.

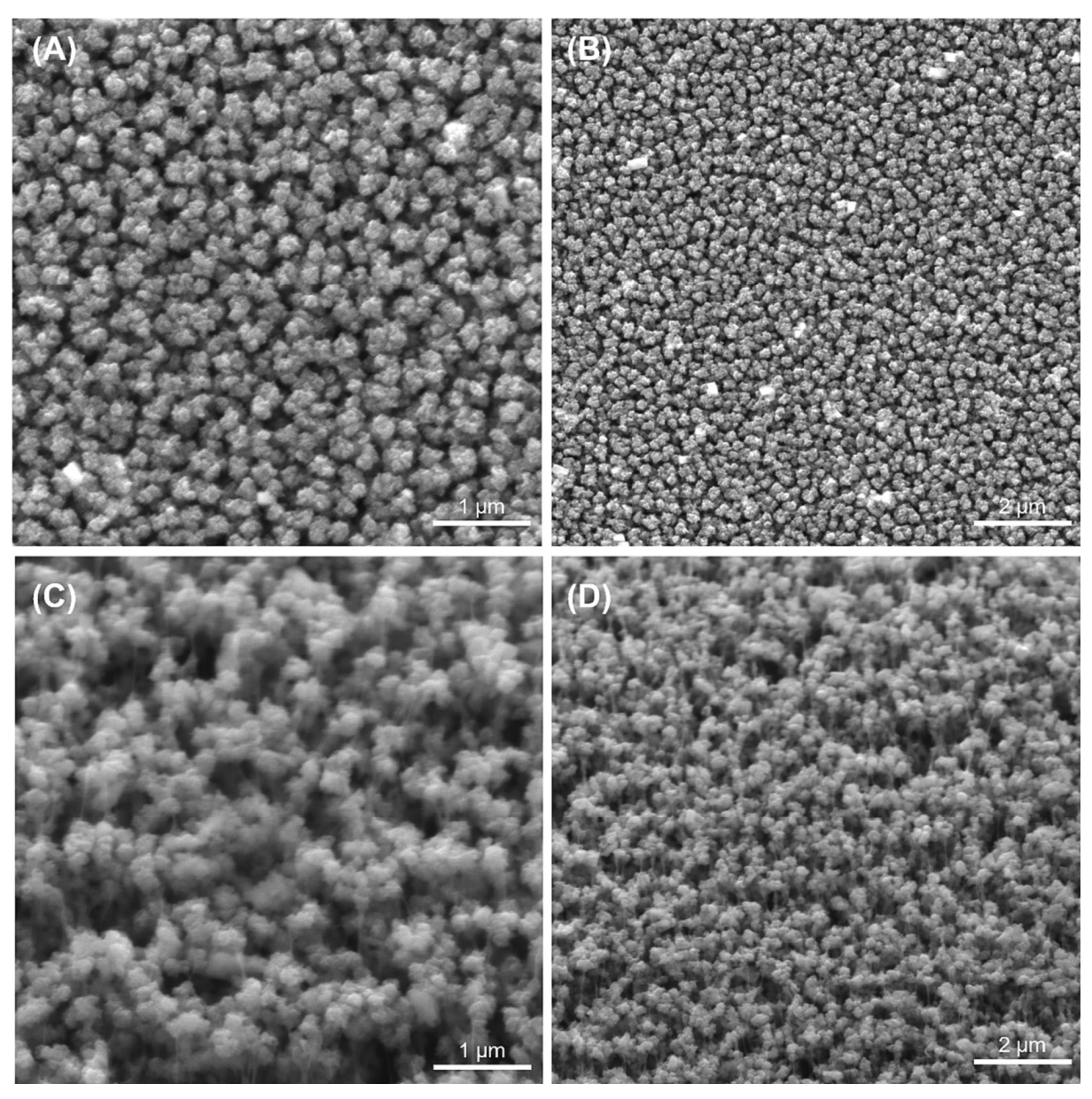


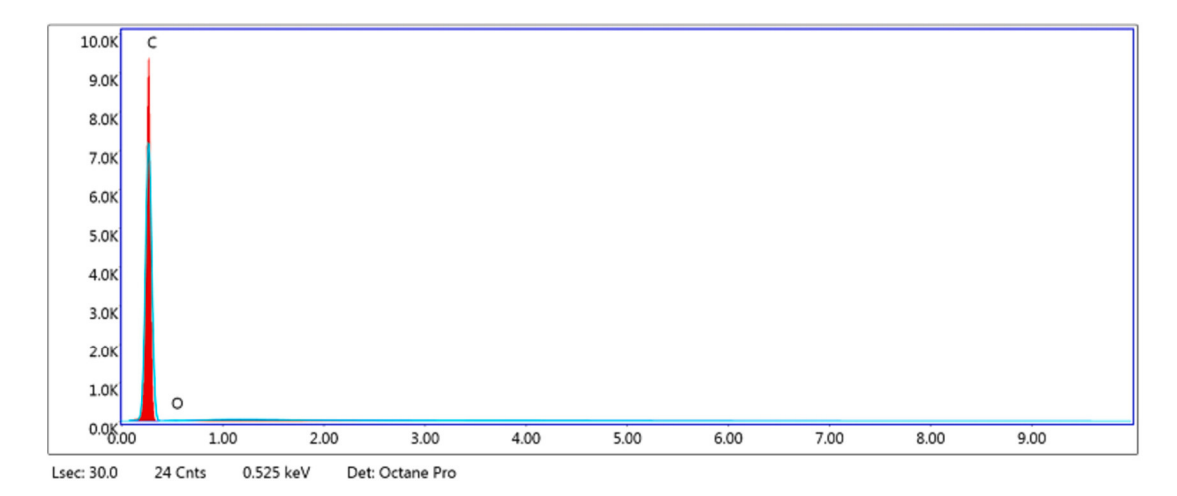
Fig. 7. SEM images of the c-PA before (A) and (B) and after (C) and (D) stretching.

d-spacings of 2.9 Å and 2.2 Å, respectively. The smaller *d*-spacings of *c*-PA indicate a slightly denser structure. This densification could be due to differences in *cis*- and *trans*- content in the films, with the *trans-l*-PA crystal unit cell being slightly smaller than *cis-l*-PA [55–57]. The cyclic topology is not expected to affect the crystal unit cell, but cyclic polymers may have larger lamellar thicknesses than their linear counterparts of similar molecular weight [58,59].

Neither of the samples have distinct peaks in their SAXS traces, likely due to the detection limit of the instrument. The large increase in intensity at q ~ 0.003 is due to the detector limit and not sample. Intensity drop-offs in SAXS scans at high q, are due to dead pixels in the detector array. c-PA appears to have a shoulder-like peak around $0.01~\text{Å}^{-1}$, which corresponds to $\sim\!63~\text{nm}$. This occurrence could be a result of the lamellar thickness of the crystal, but the feature is difficult to assign without knowing the percent crystallinity and position of the peak maximum. The l-PA shows a potentially larger lamellar thickness as there is no peak or shoulder seen in SAXS2 or SAXS3, and the decrease in intensity with q appears more linear on the log-log scale rather than exponential. There are no changes to crystal structure (WAXS) or lamellar thickness (SAXS)

for either sample under strain as the SAXS patterns overlap for all strains examined herein (Fig. 10).

The influence of stretching on the electrical resistivity of *l*-PA films has been extensively discussed in the literature [28-35,60,61]. Increasing the stretching ratios and lowering defect concentration within the l-PA films contributes to the high conductivities [29,33,62,63]. Naarmann and Theophilou added *n*-butyllithium to produce a highly uniform l-PA film with $1/l_o = 5$ and demonstrated electrical conductivity exceeding 10⁵ S/cm after doping with I₂ [33]. Tsukamoto et al. stretched l-PA films up to 5-fold and observed a 10-fold increase in conductivity to 10⁵ S/cm with FeCl₃ [36]. To explore a similar effect on c-PA films, stretching experiments were conducted and compared with cis/trans-l-PA and trans-l-PA films. The quantification of doped I2 involved weighing the polymer film both prior to and after doping. The final composition percentage was then derived by dividing the resulting weight difference by the molecular weight of iodine and comparing the moles of iodine to the moles of polyacetylene. Upon stretching the c-PA films by hand, a significant increase in conductivity was observed from 341 S/cm to 1798 S/cm (Table 2), likely due to the



eZAF Smart Quant Results

Element	Weight %	Atomic %	Net Int.	Error %	Kratio	Z	Α	F
CK	99.91	99.93	3540.67	1.51	0.9983	1.0000	0.9991	1.0000
ОК	0.09	0.07	0.83	99.99	0.0001	0.9498	0.1414	1.0000

Fig. 8. EDS of c-PA film.

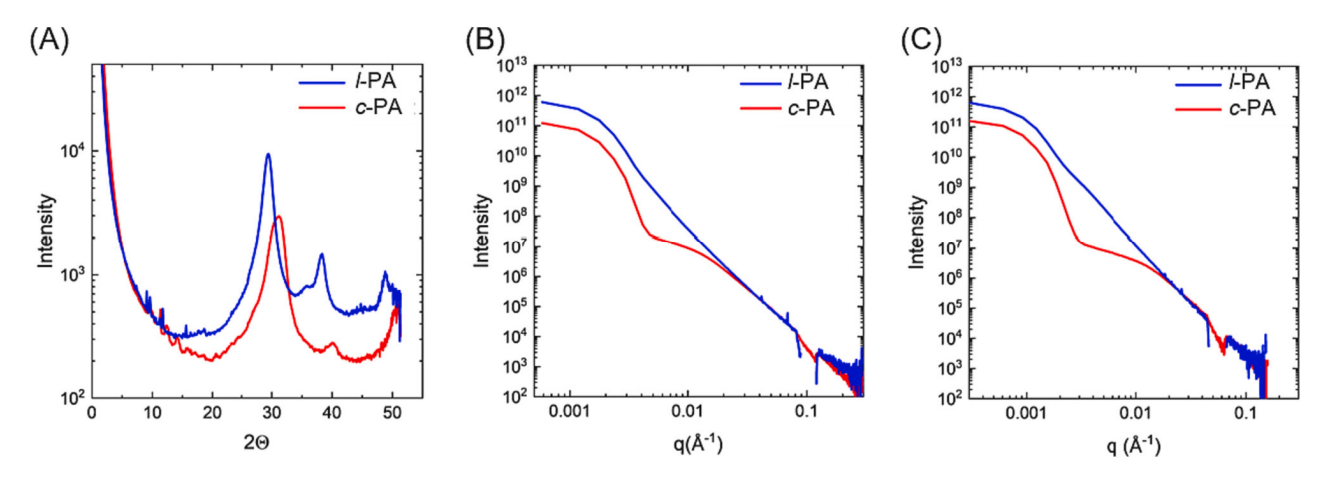


Fig. 9. X-ray scattering at 0% strain at wide-angle (WAXS) (A) small-angle distance (SAXS2) (B), and smaller-angle distance (SAXS3) (C).

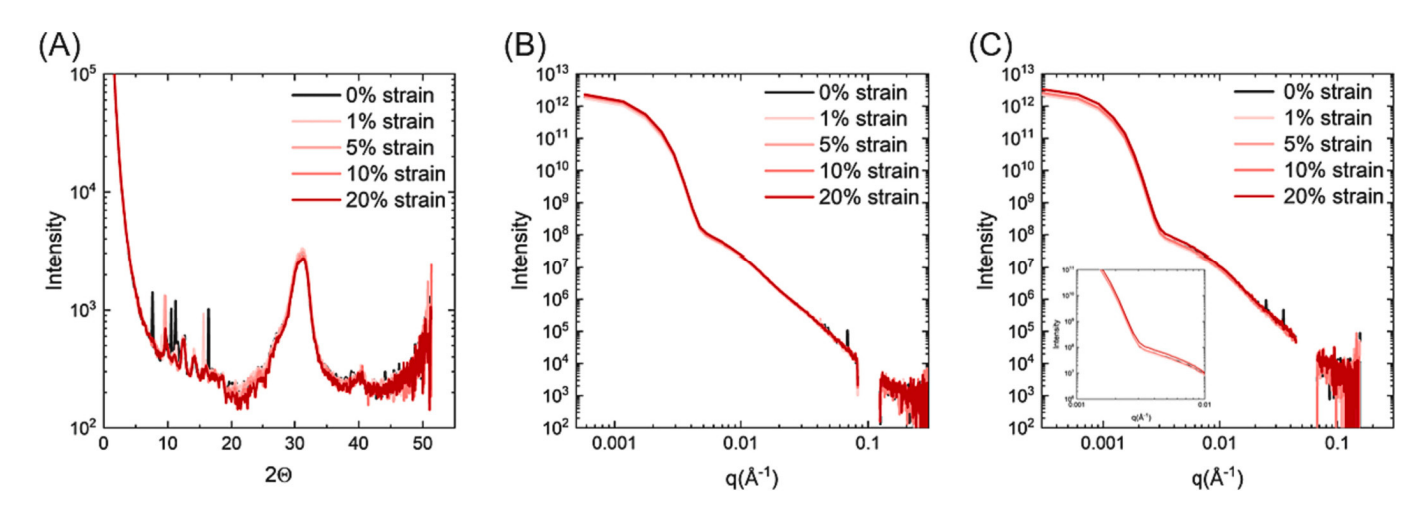


Fig. 10. X-ray scattering of c-PA at multiple strains at wide-angle (WAXS) (A) small-angle distance (SAXS2) (B), and smaller-angle distance (SAXS3) with zoomed inset (C).

Table 2 Conductivities of I_2 doped c-PA and l-PA films with different stretching procedures.

	Composition	Conductivity (S/cm)
Non-stretched c-PA	(CHI _{0.34}) _n	341 ± 25
Hand-stretched c-PA	$(CHI_{0.31})_n$	1798 ± 57
DMA-stretched c-PA	$(CHI_{0.25})_n$	1500 ± 64
Non-stretched cis/trans-l-PA	$(CHI_{0.24})_n$	209 ± 62
Hand-stretched cis/trans-l-PA	$(CHI_{0.30})_n$	227 ± 52
Non-stretched trans-l-PA	$(CHI_{0.27})_n$	524 ± 48
Hand-stretched trans-l-PA	$(CHI_{0.28})_n$	485 ± 65

improved alignment of the polyacetylene fibrils. Additionally, the conductivity reached 1500 S/cm for DMA stretched c-PA. In contrast, the conductivity of both cis/trans-l-PA and trans-l-PA films remains unchanged when hand-stretched at ambient temperature. Because these films were stretched without heating, no significant change in length occurred, resulting in no conductivity change. The conductivity values for cis/trans-l-PA and trans-l-PA films remained at 227 S/cm and 485 S/cm, respectively.

4. Conclusion

This report presents a simplified method for synthesizing thick and flexible cyclic polyacetylene films. Compared to linear polyacetylene, our approach offers several advantages, including a straightforward purification technique and stretch alignment at room temperature. Thicker films are accessible by increasing the solvent quantity during synthesis. Preliminary conductivity measurements of iodine-doped c-PA films indicate that stretching by $1.6\times$ leads to a 5-fold increase in conductivity. Our findings shed light on the distinctive properties of cyclic polyacetylene and present promising avenues for developing high-conductivity materials through a simplified and scalable approach. Unique to the synthesis of cyclic polyacetylene by catalyst 1 is the formation of the *trans*-isomer without the need to isomerize at elevated temperatures. Access to *trans-c*-PA via REP provides low defect material, including the possibility of low-cross link densities, thus yielding a more flexible material that can be stretched by hand at low temperatures.

CRediT authorship contribution statement

Yu-Hsuan Shen: Conceptualization, Formal analysis, Investigation, Methodology, Writing – original draft. Rinku Yadav: Methodology. Alexander J. Wong: Data curation, Formal analysis, Methodology. Alex H. Balzer: Data curation, Formal analysis, Validation. Thomas H. Epps: Resources, Validation, Writing – review & editing. Brent S. Sumerlin: Funding acquisition, Supervision, Writing – review & editing. Adam S. Veige: Conceptualization, Funding acquisition, Investigation, Project administration, Supervision, Writing – original draft.

Declaration of Competing Interest

ASV, BSS, and the University of Florida Research Foundation have filed patents covering the synthesis of cyclic polyacetylene and catalyst 1.

Data availability

Data will be made available on request.

Acknowledgments

The primary material synthesis and characterization efforts were supported by a National Science Foundation Award (CHE-2108266) to ASV and BSS. Microstructure characterization activities were supported by the Center for Plastics Innovation, an Energy Frontier Research

Center funded by the U.S. Department of Energy, Office of Science, Basic Energy Sciences, under award DE-SC0021166.

References

- G. Natta, G. Mazzanti, P. Corradini, Polimerizzazione stereospecifica dell'acetilene, Atti. Accad. Naz. Lincei Cl. Sci. Fis. Mat. Nat. Rend. 25 (1958) 3–12. http://www.giulionatta.it/pdf/pubblicazioni/00296.pdf.
- [2] H. Shirakawa, S. Ikeda, Infrared spectra of poly(acetylene), Polym. J. 2 (1971) 231–244, https://doi.org/10.1295/polymj.2.231.
- [3] T. Ito, H. Shirakawa, S. Ikeda, Simultaneous polymerization and formation of polyacetylene film on the surface of concentrated soluble Ziegler-type catalyst solution, J. Polym. Sci. A Polym. Chem. 34 (1996) 2533–2542, https://doi.org. 10.1002/POLA 1996-854
- [4] J. Tsukamoto, A. Takahashi, Synthesis and electrical properties of polyacetylene yielding conductivity of 105 S/cm, Synth. Met. 41 (1991) 7–12, https://doi.org/ 10.1016/0379-6779(91)90985-E.
- [5] N. Basescu, Z.X. Liu, D. Moses, A.J. Heeger, H. Naarmann, N. Theophilou, High electrical conductivity in doped polyacetylene, Nature 327 (1987) 403–405, https://doi.org/10.1038/327403a0.
- [6] C.K. Chiang, M.A. Druy, S.C. Gau, A.J. Heeger, E.J. Louis, A.G. MacDiarmid, Y. W. Park, H. Shirakawa, Synthesis of highly conducting films of derivatives of polyacetylene, (CH)x, J. Am. Chem. Soc. 100 (1978) 1013–1015, https://doi.org/10.1021/ija00471a081
- [7] C.K. Chiang, C.R. Fincher, Y.W. Park, A.J. Heeger, H. Shirakawa, E.J. Louis, S. C. Gau, A.G. MacDiarmid, Electrical conductivity in doped polyacetylene, Phys. Rev. Lett. 39 (1977) 1098–1101, https://doi.org/10.1103/PhysRevLett.39.1098.
- [8] Y.W. Park, C. Park, Y.S. Lee, C.O. Yoon, H. Shirakawa, Y. Suezaki, K. Akagi, Electrical conductivity of highly-oriented-polyacetylene, Solid State Commun. 65 (1988) 147–150, https://doi.org/10.1016/0038-1098(88)90675-8.
- [9] Y.W. Park, A.J. Heeger, M.A. Druy, A.G. MacDiarmid, Electrical transport in doped polyacetylene, J. Chem. Phys. 73 (1980) 946–957, https://doi.org/10.1063/ 1.440214
- [10] A.J. Heeger, Semiconducting and metallic polymers: the fourth generation of polymeric materials, J. Phys. Chem. B 105 (2001) 8475–8491. https://pubs.acs. org/doi/10.1021/jp011611w.
- [11] F.C. Lavarda, D.S. Galvo, B. Laks, Extended states in finite one-dimensional, disordered, highly doped, ItransR-polyacetylene chains, Phys. Rev. B 45 (1992) 3107–3110. https://doi.org/10.1103/PhysRevB.45.3107.
- [12] Y.W. Park, W.K. Han, C.H. Choi, H. Shirakawa, Metallic nature of heavily doped polyacetylene derivatives: Thermopower, Phys. Rev. B 30 (1984) 5847–5853, https://doi.org/10.1103/PhysRevB.30.5847.
- [13] J.J. Ritsko, Core excitons in Polyacetylene: evidence for a closed-gap metallic state, Phys. Rev. Lett. 46 (1981) 849–852. https://doi.org/10.1103/PhysRevLett.46.849.
- [14] C.K. Chiang, Y.W. Park, A.J. Heeger, H. Shirakawa, E.J. Louis, A.G. MacDiarmid, Conducting polymers: halogen doped polyacetylene, J. Chem. Phys. 69 (1978) 5098-5104. https://doi.org/10.1063/1.436503
- [15] C.R. Fincher, M. Ozaki, M. Tanaka, D. Peebles, L. Lauchlan, A.J. Heeger, A. G. MacDiarmid, Electronic structure of polyacetylene: optical and infrared studies of undoped semiconducting (CH) x and heavily doped metallic (CH) x, Phys. Rev. B 20 (1979) 1589–1602, https://doi.org/10.1103/PhysRevB.20.1589.
- [16] F.C. Lavarda, M.C. Dos Santos, D.S. Galv, B. Laks, Insulator-to-metal transition in polythiophene, Phys. Rev. B 49 (1994) 979–983, https://doi.org/10.1103/ PhysRevB.49.979.
- [17] E.J. Mele, M.J. Rice, Semiconductor-metal transition in doped polyacetylene, Phys. Rev. B 23 (1981) 5397–5412, https://doi.org/10.1103/PhysRevB.23.5397.
- [18] Z. Miao, D. Konar, B.S. Sumerlin, A.S. Veige, Soluble polymer precursors via ringexpansion metathesis polymerization for the synthesis of cyclic polyacetylene, Macromolecules. 54 (2021) 7840–7848. https://pubs.acs.org/doi/10.1021/acs.ma cromol.1c00938.
- [19] D.C. Bott, C.K. Chai, J.H. Edwards, W.J. Feast, R.H. Friend, M.E. Horton, A new form of polyacetylene, J. Phys. Colloques 44 (1983) 143–146, https://doi.org/ 10.1051/JPHYSCOL:1983327.
- [20] J.H. Edwards, W.J. Feast, D.C. Bott, New routes to conjugated polymers: 1. A two step route to polyacetylene, Polymer 25 (1984) 395–398, https://doi.org/ 10.1016/0032-3861(84)90293-3.
- [21] D.C. Bott, C.S. Brown, C.K. Chai, N.S. Walker, W.J. Feast, P.J.S. Foot, P.D. Calvert, N.C. Billingham, R.H. Friend, Durham poly acetylene: preparation and properties of the unoriented material, Synth. Met. 14 (1986) 245–269, https://doi.org/ 10.1016/00270.67770(8):00001.
- [22] J. Seo, S.Y. Lee, C.W. Bielawski, Unveiling a masked polymer of dewar benzene reveals trans-poly(acetylene), Macromolecules. 52 (2019) 2923–2931. https://p ubs.acs.org/doi/10.1021/acs.macromol.8b02754.
- [23] Z. Chen, J.A.M. Mercer, X. Zhu, J.A.H. Romaniuk, R. Pfattner, L. Cegelski, T. J. Martinez, N.Z. Burns, Y. Xia, Mechanochemical unzipping of insulating polyladderene to semiconducting polyacetylene, Science 357 (2017) 475–479. htt ps://www.science.org/doi/10.1126/science.aan2797.
- [24] T.M. Swager, D.A. Dougherty, R.H. Grubbs, Strained rings as a source of unsaturation: Polybenzvalene, a new soluble polyacetylene precursor, J. Am. Chem. Soc. 110 (1988) 2973–2974. https://pubs.acs.org/doi/10.1021/ja00217a 049
- [25] S. Wang, Q. Sun, O. Gröning, R. Widmer, C.A. Pignedoli, L. Cai, X. Yu, B. Yuan, C. Li, H. Ju, J. Zhu, P. Ruffieux, R. Fasel, W. Xu, On-surface synthesis and characterization of individual polyacetylene chains, Nat. Chem. 11 (2019) 924–930, https://doi.org/10.1038/s41557-019-0316-8.

- [26] Z. Miao, S.A. Gonsales, C. Ehm, F. Mentink-Vigier, C.R. Bowers, B.S. Sumerlin, A. S. Veige, Cyclic polyacetylene, Nat. Chem. 13 (2021) 792–799, https://doi.org/10.1038/s41557-021-00713-2.
- [27] C.D. Roland, H. Li, K.A. Abboud, K.B. Wagener, A.S. Veige, Cyclic polymers from alkynes, Nat. Chem. 8 (2016) 791–796, https://doi.org/10.1038/nchem.2516.
- [28] J. Płocharski, W. Pukacki, S. Roth, Electrical conductivity of iodine doped oriented polyacetylene, Synth. Met. 41 (1991) 133–136, https://doi.org/10.1016/0379-6779(91)91019-7.
- [29] Y.W. Park, C. Park, Y.S. Lee, C.O. Yoon, H. Shirakawa, Y. Suezaki, K. Akagi, Electrical conductivity of highly-oriented-polyacetylene, Solid State Commun. 65 (1988) 147–150, https://doi.org/10.1016/0038-1098(88)90675-8.
- [30] S. Matsushita, K. Akagi, Macroscopically aligned graphite films prepared from iodine-doped stretchable polyacetylene films using morphology-retaining carbonization, J. Am. Chem. Soc. 137 (2015) 9077–9087. https://pubs.acs.org/ doi/full/10.1021/jacs.5b04012.
- [31] K. Akagi, K. Sakamaki, H. Shirakawa, H. Kyotani, Polyacetylene films prepared by intrinsic non-solvent polymerization method - mechanical properties and electrical conductivities, Synth. Met. 69 (1995) 29–30, https://doi.org/10.1016/0379-6779 (94)02349-4
- [32] Y. Cao, P. Smith, A.J. Heeger, Mechanical and electrical properties of highly oriented polyacetylene films, Synth. Met. 41 (1991) 181–184, https://doi.org/ 10.1016/0379-6779(91)91033-7.
- [33] H. Naarmann, N. Theophilou, New process for the production of metal-like, stable polyacetylene, Synth. Met. 22 (1987) 1–8, https://doi.org/10.1016/0379-6779 (87)90564-9
- [34] H. Shirakawa, T. Ito, S. Ikeda, Electrical properties of polyacetylene with various cis-trans compositions, Makromol. Chem. 179 (1978) 1565–1573, https://doi.org/ 10.1002/macp.1978.021790615.
- [35] H. Shirakawa, Synthesis and characterization of highly conducting polyacetylene,
- Synth. Met. 69 (1995) 3–8, https://doi.org/10.1016/0379-6779(94)02340-5.
 [36] J. Tsukamoto, A. Takahashi, K. Kawasaki, Structure and electrical properties of Polyacetylene yielding a conductivity of 105S/cm, Jpn. J. Appl. Phys. 29 (1990) 125–130. https://iopscience.iop.org/article/10.1143/JJAP.29.125.
- [37] S. Sarkar, K.P. McGowan, S. Kuppuswamy, I. Ghiviriga, K.A. Abboud, A.S. Veige, An OCO 3- trianionic pincer tungsten(VI) alkylidyne: rational design of a highly active alkyne polymerization catalyst, J. Am. Chem. Soc. 134 (2012) 4509–4512. https://pubs.acs.org/doi/10.1021/ja2117975.
- [38] S.S. Nadif, T. Kubo, S.A. Gonsales, S. VenkatRamani, I. Ghiviriga, B.S. Sumerlin, A. S. Veige, Introducing "ynene" metathesis: ring-expansion metathesis polymerization leads to highly Cis and Syndiotactic cyclic polymers of Norbornene, J. Am. Chem. Soc. 138 (2016) 6408–6411. https://pubs.acs.org/doi/10.1021/jacs6b03247
- [39] K.P. McGowan, M.E. O'Reilly, I. Ghiviriga, K.A. Abboud, A.S. Veige, Compelling mechanistic data and identification of the active species in tungsten-catalyzed alkyne polymerizations: conversion of a trianionic pincer into a new tetraanionic pincer-type ligand, Chem. Sci. 4 (2013) 1145–1155, https://doi.org/10.1039/ C28C21250C
- [40] Y. Tezuka, Topological polymer chemistry: Progress of cyclic polymers in syntheses, Prop. Funct. 2 (2013) 1–352, https://doi.org/10.1142/8443.
- [41] Y.A. Chang, R.M. Waymouth, Recent progress on the synthesis of cyclic polymers via ring-expansion strategies, J. Polym. Sci. A Polym. Chem. 55 (2017) 2892–2902, https://doi.org/10.1002/POLA.28635.
- [42] C.W. Bielawski, D. Benitez, R.H. Grubbs, An "endless" route to cyclic polymers, Science 297 (2002) 2041–2044. https://www.science.org/doi/10.1126/science.1 075401.
- [43] S.A. Gonsales, T. Kubo, M.K. Flint, K.A. Abboud, B.S. Sumerlin, A.S. Veige, Highly tactic cyclic Polynorbornene: Stereoselective ring expansion metathesis polymerization of Norbornene catalyzed by a new tethered tungsten-Alkylidene catalyst, J. Am. Chem. Soc. 138 (2016) 4996–4999. https://pubs.acs.org/doi/10.1021/jacs.6b00014.
- [44] Y. Xia, A.J. Boydston, Y. Yao, J.A. Kornfield, I.A. Gorodetskaya, H.W. Spiess, R. H. Grubbs, Ring-expansion metathesis polymerization: catalyst-dependent

- polymerization profiles, J. Am. Chem. Soc. 131 (2009) 2670–2677. https://pubs.acs.org/doi/10.1021/ja808296a.
- [45] J.C.W. Chien, G.E. Wnek, F.E. Karasz, J.A. Hirsch, Electrically conducting acetylene-Methylacetylene copolymers, Synthesis Prop. Macromol. 14 (1981) 479–485, https://pubs.acs.org/doi/10.1021/ma50004a004.
- [46] G.E. Wnek, Synthesis and properties of electrically conducting polymers, Doctoral Dissertations 1980 (1896) 656–965, https://doi.org/10.7275/k31e-qg53.
- [47] A.G. MacDiarmid, A.J. Heeger, Organic metals and semiconductors: the chemistry of Polyacetylene, (CH)x, and its derivatives, The Physics and Chemistry of Low Dimensional Solids 56 (1980) 393–402, https://doi.org/10.1007/978-94-009-0067-8-24
- [48] A.M. Saxman, R. Liepins, M. Aldissi, Polyacetylene: its synthesis, doping and structure, Prog. Polym. Sci. 11 (1985) 57–89, https://doi.org/10.1016/0079-6700
- [49] H. Shirakawa, S. Ikeda, Infrared spectra of poly(acetylene), Polym. J. 2 (1971) 231–244, https://doi.org/10.1295/polymj.2.231.
- [50] A.G. MacDiarmid, A.J. Heeger, Organic metals and semiconductors: the chemistry of polyacetylene, (CH)x, and its derivatives, Synth. Met. 1 (1980) 101–118, https://doi.org/10.1016/0379-6779(80)90002-8.
- [51] H. Shirakawa, S. Ikeda, Preparation and morphology of as-prepared and highly stretch-aligned polyacetylene, Synth. Met. 1 (1980) 175–184, https://doi.org/ 10.1016/0379-6779(80)90008-9.
- [52] M.A. Druy, C.H. Tsang, N. Brown, A.J. Heeger, A.G. MacDiarmid, Tensile properties and partial alignment of polyacetylene, (CH)x, films, J. Polym. Sci. 18 (1980) 429–441. https://doi.org/10.1002/POL1980.180180303.
- [53] A.M. Saxman, R. Liepins, M. Aldissi, Polyacetylene: its synthesis, doping and structure, Prog. Polym. Sci. 11 (1985) 57–89, https://doi.org/10.1016/0079-6700 (85)00008-5
- [54] D.S. Jones, Dynamic mechanical analysis of polymeric systems of pharmaceutical and biomedical significance, Int. J. Pharm. 179 (1999) 167–178, https://doi.org/ 10.1016/S0378-5173(98)00337-8.
- [55] J.C.W. Chien, M.A. Schen, Low- and high-molecular-weight polyacetylenes: synthesis, characterization, and thermal isomerization, J. Polym. Sci., Polym. Chem. Ed. 23 (1985) 2447–2459, https://doi.org/10.1002/POL.1985.170230910.
- [56] G. Perego, G. Lugli, U. Pedretti, M. Cesari, X-ray investigation on highly oriented polyacetylene, 1. Crystal structure of cis- and trans-polyacetylene, Die Makromolekulare Chemie. 189 (1988) 2657–2669, https://doi.org/10.1002/ macp.1988.021891113.
- [57] G. Perego, G. Lugli, U. Pedretti, M. Cesari, X-ray investigation on highly oriented polyacetylene, 2. Crystal structure of cis- and trans-polyacetylene, Die Makromolekulare Chemie 189 (1988) 2671–2686, https://doi.org/10.1002/ macp.1988.021891114.
- [58] N. Zaldua, R. Liénard, T. Josse, M. Zubitur, A. Mugica, A. Iturrospe, A. Arbe, J. De Winter, O. Coulembier, A.J. Müller, Influence of chain topology (cyclic versus linear) on the nucleation and isothermal crystallization of poly(1-lactide) and poly (d-lactide), Macromolecules. 51 (2018) 1718–1732, https://doi.org/10.1021/acs.macromol/7b02638
- [59] H.H. Su, H.L. Chen, A. Díaz, M.T. Casas, J. Puiggalí, J.N. Hoskins, S.M. Grayson, R. A. Pérez, A.J. Müller, New insights on the crystallization and melting of cyclic PCL chains on the basis of a modified Thomson–Gibbs equation, Polymer 54 (2013) 846–859, https://doi.org/10.1016/j.polymer.2012.11.066.
- [60] Y.W. Park, A.J. Heeger, M.A. Druy, A.G. MacDiarmid, Electrical transport in doped polyacetylene, J. Chem. Phys. 73 (1980) 946–957, https://doi.org/10.1063/ 1.440214.
- [61] Y. Nogami, H. Kaneko, T. Ishiguro, A. Takahashi, J. Tsukamoto, N. Hosoito, On the metallic states in highly conducting iodine-doped polyacetylene, Solid State Commun. 76 (1990) 583–586, https://doi.org/10.1016/0038-1098(90)90093-Q.
- [62] N. Basescu, Z.X. Liu, D. Moses, A.J. Heeger, H. Naarmann, N. Theophilou, High electrical conductivity in doped polyacetylene, Nature 327 (1987) 403–405, https://doi.org/10.1038/327403a0.
- [63] A.G. MacDiarmid, A.J. Heeger, Organic metals and semiconductors: the chemistry of polyacetylene, (CH)x, and its derivatives, Synth. Met. 1 (1980) 101–118, https://doi.org/10.1016/0379-6779(80)90002-8.